Hydroacoustic interaction between draft tube and penstock eigenmodes under Francis turbine full load instability

S. Alligné[1], C. Nicolet[1]; Y. Vaillant[2], P-Y. Lowys[3], J. Heraud[4]; B. Lecomte[5]
[1] Power Vision Engineering Sàrl, St-Sulpice, Switzerland
[2] Principal Engineer, Hydraulic Transients, GE Renewable Energy Hydro Solutions, Birr, Switzerland
[3] Chief Consulting Engineer, Turbine, GE Renewable Energy Hydro Solutions, Brossard, Canada
[4] Hydromechanics Engineer, EDF DTG, Grenoble, France
[5] Senior Engineer, EDF DTG, Grenoble, France

Abstract. At high load, Francis Turbines may experience self-sustained pressure surge leading to significant power swing and pressure fluctuations along the waterway. The physical mechanism initiating this instability phenomenon has been the subject of much research. The development of the axisymmetric cavitating vortex rope at the runner outlet modifies the hydroacoustic properties of the draft tube waterway. Very low wave speed due to high cavitation volume combined with a high swirling number initiates the unstable axial pulsations of the cavitating vortex rope which frequency corresponds to a penstock's eigenfrequency. The 15 MW power plant of Monceaux-la-Virole in France, composed of two units fed by a single penstock, experiences such full-load surge. On-site tests have been carried out to analyze the envelope of pressure fluctuations along the penstock once instability occurs. Combined with a 1D SIMSEN model of the power plant, these measurements have allowed to enhance the understanding of this instability phenomenon. To achieve this, an advanced draft tube modelling taking into account distributed wave speed, convective terms and divergent geometry is used and frequency analysis is carried out. Unstable draft tube eigenmodes and stable penstock eigenmodes are predicted. The key draft tube model parameters such as wave speed and second viscosity are calibrated to set the draft tube eigenmode frequency to the unstable measured frequency for different operating points. This frequency analysis concludes that high load instability occurs when a matching between the draft tube and the penstock eigenfrequencies is experienced. Moreover, it is shown that the unstable draft tube eigenmode is able to interact with different order penstock eigenmodes as function of the operating point of the unit.

1. Introduction

By 2050, the high Renewable Energy Sources (RES) scenario of the decarbonisation process forecasts a 97 % share of renewable electricity in the European power generation mix. Decarbonisation will require the disconnection and decommissioning of the so-called conventional units, namely the generating units of the fossil fuel thermal power plants, as greenhouse gases emitters. Combination of increasing amount of intermittent RES and decreasing power balancing services with conventional power plants will induce much higher volatility of the Electric Power System (EPS). Hence flexibility of the existing and new electrical utilities must be increased to ensure grid balancing functionalities. Regarding the Hydroelectric Power Plants (HPP), their operation mode needs to be revised to be more flexible and to provide more ancillary services to the power grid. This translates into wider operating range of the units, where the turbine efficiency decreases drastically or flow instabilities inducing cavitation and pressure fluctuations appear, risking damage and reducing the life span of the unit.

At high load, Francis Turbines may experience self-sustained pressure surge leading to significant power swing and pressure fluctuations along the waterway. Example of hydropower plants experiencing full load surges can be found in [1]-[6]. The physical mechanism initiating this instability phenomenon has been the subject of much research. Mathematical approach [7] - [12] or numerical simulations [13] - [16] to explain the full load instability and its relation with the swirling flow under the runner can be found. The development of the axisymmetric cavitating vortex rope at the runner outlet modifies the hydroacoustic properties of the draft tube waterway. Very low wave speed due to high cavitation volume combined with a high swirling number initiates cavitating vortex rope volume fluctuations which frequency corresponds to a hydraulic system's eigenfrequency. 1D numerical models for the simulation of unstable full load conditions take into account the cavitation compliance, the second viscosity and the mass flow gain factor hydroacoustic parameters [10]. Despite all these studies and numerical models, the physical mechanism inducing the occurrence of full load instability is still unknown and needs more investigations.

The 15 MW power plant of Monceaux-la-Virole in France, composed of two Francis turbine units fed by a single penstock, experiences such full-load surge. On-site tests have been carried out to analyse the envelope of pressure fluctuations along the penstock once instability occurs [5]. In this paper, a 1D SIMSEN model of the power plant is implemented including an advanced draft tube modelling taking into account distributed wave speed, convective terms and divergent geometry. Based on this 1D model, stability analysis by computing eigenmodes of the powerplant is carried out to enhance the understanding of this instability phenomenon. Hydroacoustic parameters of the draft tube model have been calibrated to fit prediction frequencies with the measurements.

2. Full load instability experienced at Monceaux-la-Virole power plant

The full load instability phenomenon was experienced at Monceaux-la-Virole power plant in France. As shown in Figure 1, it is composed of a 3'473 m long headrace tunnel with a diameter varying from 2.36 m to 2.5 m, a differential surge tank, a 408 m long penstock with a diameter varying from 2 m to 1.8 m and two 7.5 MW Francis vertical axis units equipped with pressure relief valve.

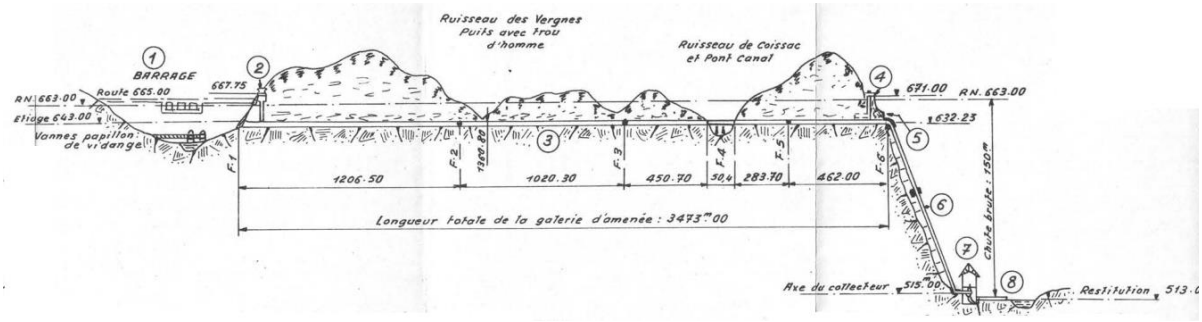

Figure 1 Hydraulic layout of the Monceaux-la-Virole power plant.

In order to characterize this high load instability phenomenon, measurements of pressure fluctuations in the spiral case and along the penstock were carried out during the loading test of one unit with the second one at standstill [5]. The Figure 2 shows a time-frequency diagram of pressure fluctuations measured at the spiral case. Three main pressure fluctuation zones are identified when the load is increased: one at part load condition and two at full load condition. Two full load operating points, OP1 and OP2 respectively at 1.16 and 1.19 times the rated output power, can be defined with a minor change in guide vane opening since they are very close in time. By changing of 2% the guide vane opening between OP1 and OP2, the unstable frequency of pressure fluctuations switches from 3.4 Hz to 2.35 Hz. Spatial representations of pressure fluctuations amplitudes along the penstock measured at 3.4 Hz for OP1 and at 2.35 Hz for OP2, are shown respectively in Figure 3 and Figure 4. The measured pressure patterns correspond to a 7/4 wave form for OP1, featuring three pressure nodes (in addition to the surge tank), and a 5/4 wave form for OP2, featuring two pressure nodes.

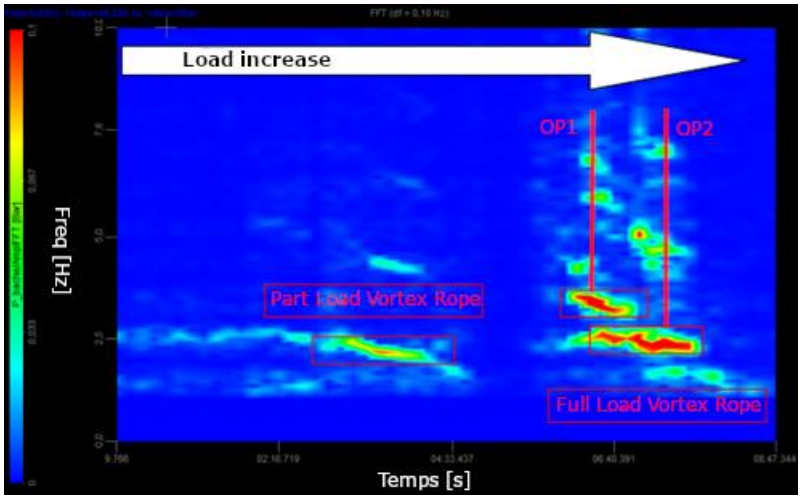

Figure 2 Time-Frequency diagram of pressure fluctuations. Evolution of pressure fluctuations as function of the turbine load increase.

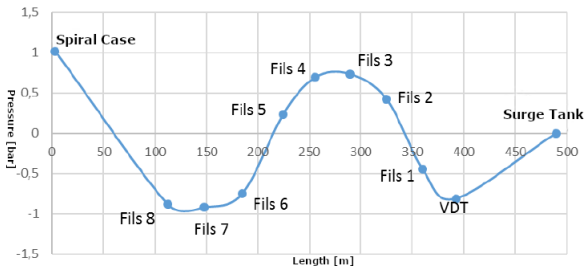

Figure 3 Pressure fluctuations amplitude along the penstock experienced at OP1 with frequency of 3.4 Hz / 21.4 rad/s (7/4 wave form).

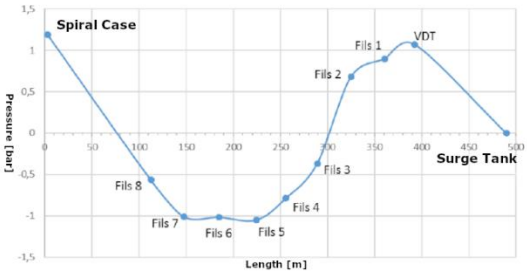

Figure 4 Pressure fluctuations amplitude along the penstock experienced at OP2 with frequency of 2.35 Hz / 14.9 rad/s (5/4 wave form).

3. Hydroacoustic modelling of power plant for stability analysis

The observed phenomenon of the switch between the two unstable frequencies between OP1 and OP2 is unusual and requires a stability analysis of the complete power plant for a better understanding. Therefore a 1D numerical model of the power plant is setup with the SIMSEN software including the headrace tunnel, the surge tank, the penstock and the hydraulic machines. In SIMSEN, hydraulic components are modelled with an electrical analogy and pipe elements can be modelled with a "T-shaped" equivalent electrical scheme [17]. Fluid compressibility, fluid inertia and energy losses are represented, respectively, by a capacitance C_c, an inductance L and a resistance R_λ:

$$C_c = \frac{g \cdot A \cdot dx}{a^2};\ L = \frac{dx}{g \cdot A};\ R_\lambda = \frac{\lambda \cdot |\bar{Q}| \cdot dx}{2 \cdot g \cdot D \cdot A^2} \quad (1)$$

The modelling of the draft tube differs from a standard pipe model because of its divergent geometry and the presence of cavitation which yields to low wave speed values. Consequently, additional electrical components are considered in the equivalent electrical scheme for such component as shown in Figure 5 [10]. First, the divergent geometry inducing the increase of pressure along the draft tube is modelled through a negative resistance $-R_d$. Then, due to low wave speed values, convective terms cannot be neglected anymore and are modelled with a voltage source J. Moreover, dissipation induced by cavitation volume fluctuations is represented by a resistance R_μ in series with the capacitance. Finally, influence of the inlet swirling flow on the cavitation volume in the draft tube is modelled with the mass flow gain factor χ. According to the electrical analogy, the voltage at the terminal of the capacitances represent the pressure. A so-called distributed model is used when several pressure nodes are defined whereas if only one pressure node is set, a so-called lumped model is implemented. The

higher is the number of pressure nodes, the higher is the frequency of phenomena that can be predicted. In the case of this study, the number of pressure nodes in the draft tube cone is set to 10 and comparison with lumped model is performed as well.

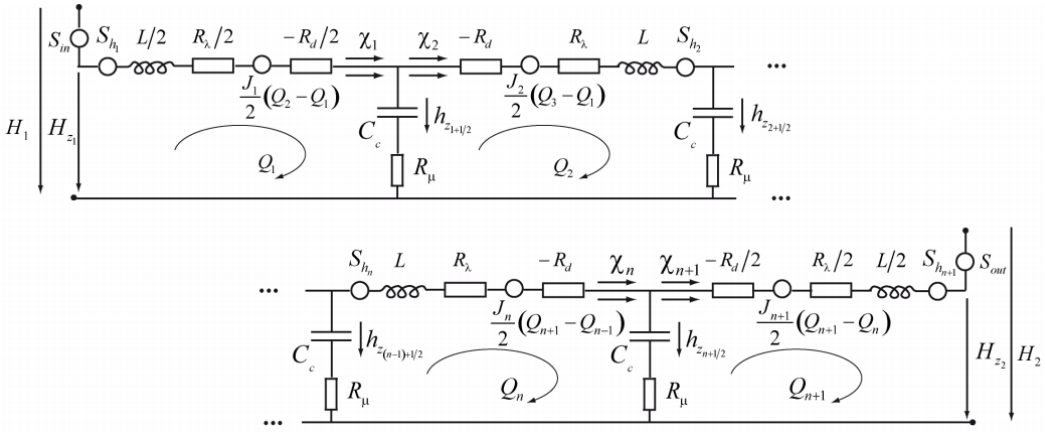

Figure 5 Distributed draft tube model.

4. Hydroacoustic interaction between draft tube and penstock eigenmodes

4.1. Draft tube and penstock eigenmodes

A small perturbation stability analysis of the complete hydraulic system model is carried out. This stability analysis is based on the linearization of the set of differential equations around the operating point. Then, from the linearized matrices, complex eigenvalues $s = \alpha + j\omega$ are computed. Damping and oscillation frequency of the eigenmodes are given, respectively, by the real part and the imaginary part of the eigenvalues. Positive damping corresponds to unstable eigenmode leading to self-oscillations of the hydraulic system as experienced during full load surges at OP1 and OP2. Negative damping yields to stable eigenmodes. Moreover, each complex eigenvalue is associated to a complex eigenvector which modulus and phase are used to compute time evolution of pressure and discharge fluctuations in the hydraulic system. The stability analysis has shown the co-existence of draft tube and penstock eigenmodes. Draft tube eigenmodes are characterized by high pressure fluctuation amplitudes both in the draft tube component and in the penstock. Whereas penstock eigenmodes feature high amplitudes in the penstock and low amplitudes in the draft tube. Due to the presence of cavitation in the draft tube, the wave speed drops drastically to low values and can reach up to 10 m/s. By applying this limit value in the distributed draft tube model for OP2, the predicted first four draft tube and penstock pressure eigenmodes are presented in the Figure 6. Damping and pulsation of each eigenmode are mentioned in Table 1. For all the draft tube eigenmodes, real part of the eigenvalue is positive, meaning that these eigenmodes are unstable and capable of producing self-oscillations in the hydraulic system. While all the penstock eigenmodes are stable. It is shown in Table 1 that the high order draft tube eigenmodes cannot be predicted by the lumped draft tube model since the spatial discretization is not sufficient to reproduce nodes and antinodes in the draft tube component.

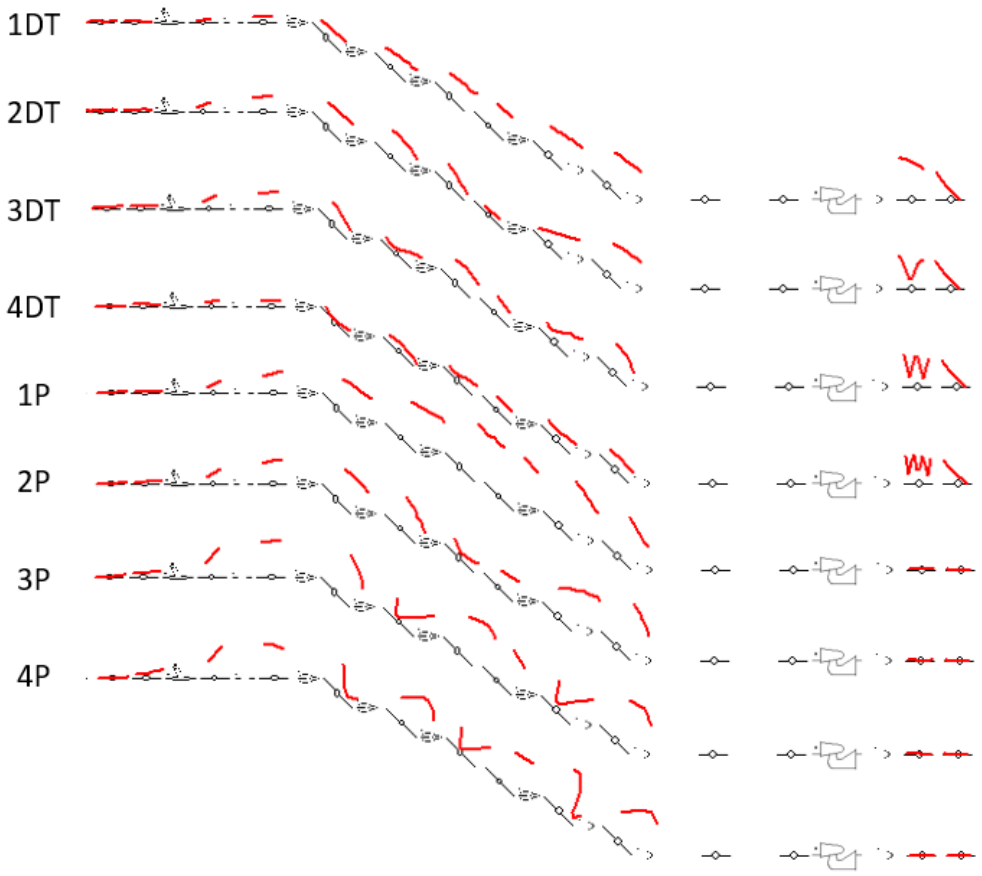

Figure 6 OP2-Shapes of draft tube (DT) and penstock (P) pressure fluctuations amplitudes of eigenmodes predicted with wave speed in the draft tube of 10 m/s.

Table 1 OP2-Dampings and pulsations of draft tube and penstock eigenmodes predicted with draft tube wave speed value of 10 m/s. Comparison between distributed and lumped draft tube models.

Mode	Distributed		Lumped	
	a=10m/s		a=10m/s	
	α	w	α	w
1DT	0,13	2,25	0,10	2,15
2DT	0,20	8,71	---	---
3DT	0,23	16,39	---	---
4DT	0,32	24,02	---	---
1P	-0,73	4,88	-0,73	4,88
2P	-0,95	10,33	-0,93	10,26
3P	-0,97	15,52	-0,97	15,49
4P	-1,40	21,52	-1,39	21,49

The draft tube eigenmode frequencies are strongly influenced by the wave speed value parameter in the draft tube model. If the measured pressure fluctuations is assumed to correspond to the self-oscillations of one of the draft tube eigenmodes, the wave speed parameter can be calibrated to match the pulsation frequency of a supposed unstable draft tube eigenmode with measurements. This calibration procedure has been performed at OP2 to match with the measured pulsation frequency value of $\omega = 15\ rad/s$. As a result, to match the first draft tube eigenmode pulsation frequency with measurement, the wave speed value should be 70 m/s. Whereas to match the second or the third draft tube eigenmode, the wave speed value should be respectively 17 m/s or 9.3 m/s. As reported in Table 2, damping and pulsation of all the eigenmodes have been computed with these three potential wave speed values. The assumption that the

first draft tube eigenmode is unstable can be discarded since the real part of the eigenvalue is negative. The two other assumptions involving the second and the third draft tube eigenmode are however possible.

Table 2 OP2-Calibration of draft tube wave speed to match draft tube eigenmode frequency with the unstable measured frequency on-site.

Mode	a=70m/s - Mode1DT		a=17m/s - Mode2DT		a=9.3m/s - Mode3DT	
	α	w	α	w	α	w
1DT	-0,48	15,07	0,12	3,79	0,12	2,09
2DT	0,05	63,66	0,14	15,18	0,21	8,06
3DT	0,23	118,53	0,23	28,51	0,24	15,14
4DT	0,32	172,06	0,32	41,52	0,31	22,25
1P	-0,67	4,79	-0,72	4,97	-0,73	4,88
2P	-0,77	10,07	-0,94	10,28	-0,96	10,31
3P	-0,52	16,95	-0,93	15,59	-0,98	15,54
4P	-1,44	21,68	-1,40	21,52	-1,40	21,52

For each wave speed assumption at OP2, the draft tube pressure eigenmode which frequency corresponds to the measurement is represented in Figure 7. One can notice that the pressure mode shape in the penstock remains unchanged whatever the order of the draft tube mode considered as unstable. The number and the location of the pressure nodes in the penstock are similar between the three assumptions. Only the frequency imposes the shape in the penstock. However, the order of the unstable draft tube eigenmode imposes the number of pressure nodes in the draft tube.

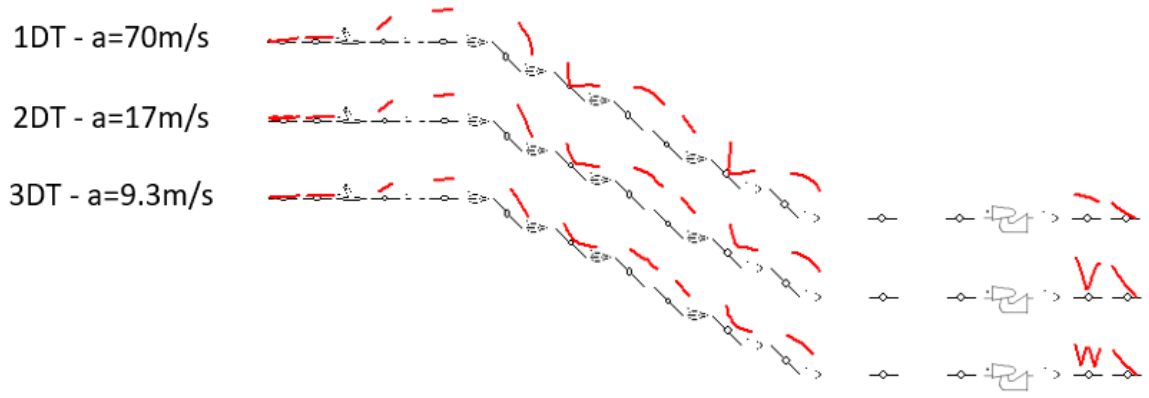

Figure 7 OP2-Shapes of draft tube pressure fluctuations amplitudes of eigenmodes with wave speed matching the unstable measured frequency of 2.35 Hz / 14.9 rad/s.

4.2. Switch of unstable frequency between OP1 and OP2

By increasing the guide vane opening of 2 % from OP1 to OP2, measurements have shown that the unstable frequency switches from 3.4 Hz to 2.35 Hz. It is assumed that the cavitation volume of the full load vortex rope in the draft tube increases and induces a decrease of the wave speed. In Figure 8, the frequencies of the draft tube eigenmodes are plotted as function of the wave speed. The measured unstable frequencies are also plotted and are represented by the horizontal lines in red for OP1 and in green for OP2. As it can be observed in the time-frequency diagram in Figure 2, pressure fluctuations measured at OP1, contain two frequency components. This is why two horizontal red lines are represented: the dominant frequency component at $\omega = 21\, rad/s$ in solid line and the secondary frequency component at $\omega = 17\, rad/s$ in dashed line. Therefore it is assumed that two draft tube eigenmodes are unstable at OP1. To identify the draft tube wave speed values at OP1 and OP2, the

intersections between horizontal lines and curves of the draft tube eigenmodes frequencies must be considered. Several solutions, listed in Table 3, have been analysed.

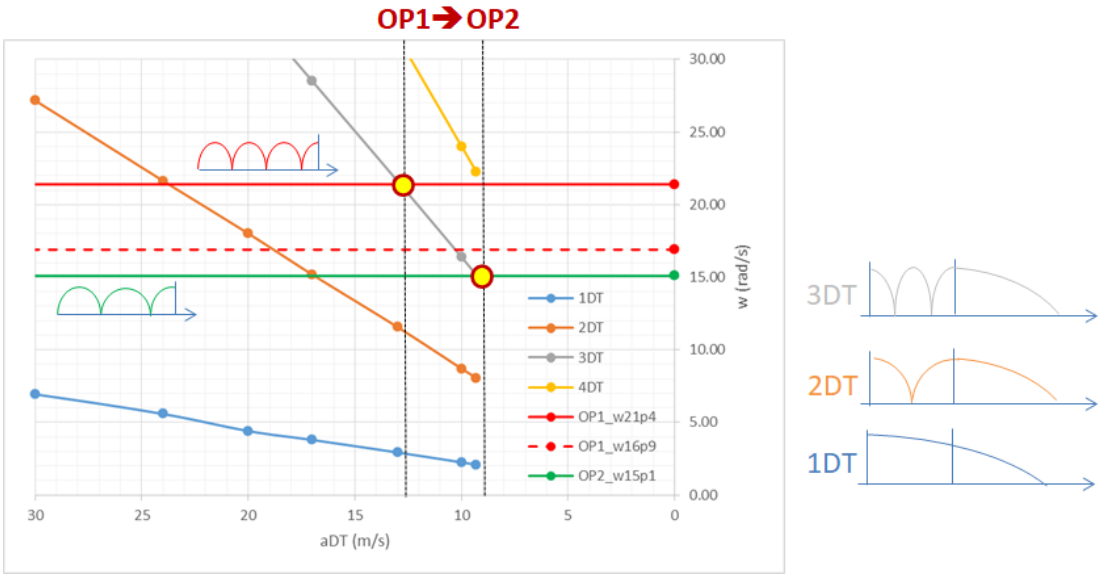

Figure 8 Draft tube mode pulsations as function of draft tube wave speed value.

To identify the adequate configuration, two criteria have been used. First, the draft tube eigenmodes must be predicted as unstable and then, the wave speed between OP1 and OP2 must decrease. Finally, the retained assumption, numbered #1 in Table 3, is that the dominant frequency at OP1 and the frequency at OP2 correspond to the same draft tube eigenmode, the third one, named 3DT. In such configuration, the wave speed decreases from 13m/s to 9.3m/s by a change of 2% of guide vane opening.

Table 3 List of assumptions to identify unstable draft tube eigenmodes at OP1 and OP2.

Assumption		OP1		OP2		Comment
Same eigenmode	#1	3DT-w21 2DT-w17	a=13m/s	3DT-w15	a=9.3m/s	Valid - Wave speed (WS) decreases
	#2	2DT-w21 1DT-w17	a=24m/s	2DT-w15	a=17m/s	Not valid - 1DT is predicted as stable and WS increases
Different eigenmode	#3	2DT-w21 1DT-w17	a=24m/s	1DT-w15	a=70m/s	Not valid - 1DT is predicted as stable and WS increases
	#4	3DT-w21 2DT-w17	a=13m/s	2DT-w15	a=17m/s	Not valid - WS increases
	#5	2DT-w21 1DT-w17	a=24m/s	3DT-w15	a=9.3m/s	Not valid - 1DT is predicted as stable at OP1

The pressure fluctuations in the penstock and in the draft tube corresponding to the assumption #1 are represented respectively in Figure 9 and in Figure 10. Pressure fluctuations experienced at the two operating points OP1 and OP2 are compared with measurements. In the penstock, the number of nodes are reproduced for both operating points and the spatial amplitude evolution is well reproduced. In the draft tube, unfortunately, only one measurement location is available and do not allow to capture the spatial shape defining the order of the unstable eigenmode. Measurements show a higher amplitude at OP2. Curves plotted in Figure 10 represent the amplitudes of the 3DT eigenmode and are compared to amplitudes of time pressure fluctuation measurements. To rebuild the time evolution of the system response from eigenmodes, eigenvectors $\overrightarrow{\varphi_i}$ and eigenvalues s_i must be considered as mentioned in

equation (2). As a result, the resulting time fluctuation amplitude depends on the real part of the eigenvalue s_i.

$$\delta\vec{X} = 2.\mathrm{Re}\left(\sum_{i=1}^{n/2}(c_i \cdot \overrightarrow{\varphi_i} \cdot e^{s_i t})\right) \quad (2)$$

The numerical model predicts relative damping values of $\alpha/\omega = +0.011$ $\alpha/\omega = +0.016$ of the 3DT eigenmode respectively for OP1 and OP2. Since positive damping corresponds to self-excitation and amplification of the system response, higher amplitudes are expected at OP2 compared to OP1 which is in good agreement with measurements.

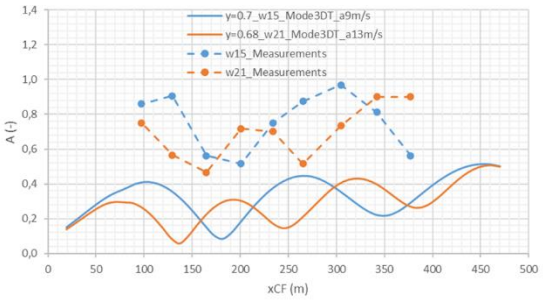

Figure 9 Assumption #1 - Pressure fluctuations amplitude 3DT along the penstock experienced at OP2 and OP1.

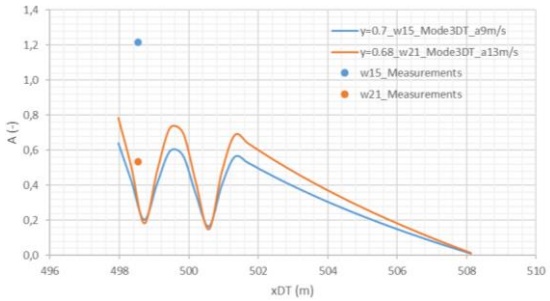

Figure 10 Assumption #1- Pressure fluctuations amplitude 3DT along the draft tube experienced at OP2 and OP1.

4.3. Interaction between draft tube and penstock eigenmodes inducing high load surge

The stability analysis has shown the existence of draft tube and penstock eigenmodes. Frequency and damping of penstock eigenmodes are not influenced by the wave speed in the draft tube, while frequency and damping of draft tube eigenmodes are dependent on this parameter. Indeed, with high wave speed values, the draft tube eigenmodes feature high frequencies and remain stable, while by decreasing the wave speed value, frequencies of draft tube eigenmodes decrease and may become unstable. On the other hand, the analysis of the pressure fluctuation measurements in the penstock show a spatial distribution corresponding to the penstock eigenmodes 4P and 3P, respectively for the operating points OP1 and OP2. However, as mentioned previously, these eigenmodes are found to be always stable whatever the wave speed value in the draft tube. These observations lead to the conclusion that the fourth penstock eigenmode 4P at OP1 and the third penstock eigenmode 3P at OP2 are self-excited by the third unstable draft tube eigenmode 3DT. A matching between penstock eigenfrequency and unstable draft tube eigenmode frequency leads to high load surge phenomenon. With this case study, this matching occurs twice with different penstock eigenmodes by increasing the turbine load.

5. Calibration of stability limits

By increasing the guide vane opening of 2% from OP1 to OP2, the wave speed decreases from 13m/s to 9.3m/s. With such low wave speed values, the model predicts all the draft tube eigenmodes as unstable with positive real part of the eigenvalue. This is induced by the divergent geometry of the draft tube combined with low wave speed values [9], **Erreur ! Source du renvoi introuvable.**], [10]. However, some of the draft tube eigenmodes should be predicted as stable since the time-frequency diagram in Figure 2, shows only two and one unstable frequencies respectively at OP1 and OP2. To make some of the draft tube eigenmodes stable, the damping which defines the resistance in series with the capacitance in the equivalent electrical scheme presented in Figure 5, must be considered. The second viscosity parameter μ'' ,defining this resistance, is known as dependent on frequency phenomena [18]. It is used both in case of cavitation-free pipe modelling and of draft tube modelling to consider energy dissipation due to cavitation vortex rope volume fluctuations [10]. For this stability analysis, the second viscosity in the penstock has been calibrated to $\mu'' = 2.10^7 Pa.s$ to fit with measurements of the damping of pressure fluctuations amplitude induced by water hammer featuring a frequency of $f = 0.5\ Hz$. In the

draft tube, this parameter has been calibrated as function of frequency to define the stability limit of each draft tube eigenmode, i.e the real part of the eigenvalue near to zero. The Figure 11 shows the stability limit found for the two operating points in terms of second viscosity μ''as function of frequency. For OP1, the second viscosity parameter is calibrated to define stability limit giving only the eigenmodes 3DT and 2DT as unstable. Whereas at OP2, the second viscosity parameter is calibrated to get only the eigenmode 3DT as unstable.

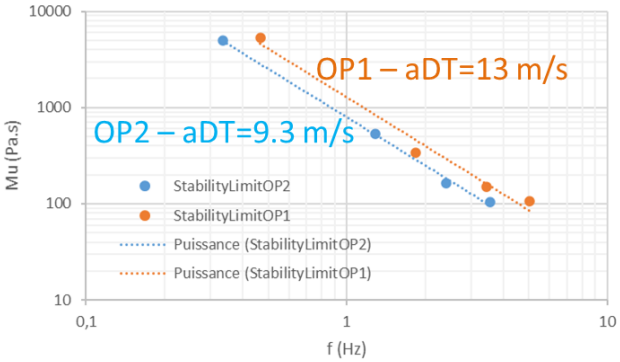

Figure 11 Calibration of second viscosity parameter to define stability limit for OP1 and OP2.

6. Influence of a static air sheet at the bottom of the penstock

Air injection tests near the penstock protection valve were conducted to reduce pressure fluctuations in the penstock due to high load instability. Among all these tests, one of them has allowed to consolidate the predictions of the numerical model and the assumption retained to explain the nature of the measured pressure fluctuations. Figure 12 presents the scenario of the test showing the influence of a static air sheet located at the bottom of the penstock. This scenario presents five major events:

- Event #1: the unit 1 is running at OP1 and the unit 2 is at standstill with the main inlet valve closed. In such condition, high load instability is experienced with unit 1 with pressure fluctuations measured in the spiral case;
- Event #2: the main inlet valve of the unit 2 is opened which highly reduces pressure fluctuations in the system;
- Event#3: start-up of the unit 2. The measured pressure fluctuations are still reduced;
- Event#4: stop of the unit 2 with closure of the main inlet valve. By closing the valve, the high load instability is back;
- Event#5: the main inlet valve of the unit 2 is re-opened. Contrary to the Event#2, the high load instability does not disappear.

The observation of these events yields to the following explanation. Due to several air injection tests, air volume has been captured downstream of the main inlet valve of unit 2 which is initially closed at the beginning of the scenario. When the main inlet valve of unit 2 is opened, the air volume is subjected to the pressure fluctuations of the high load instability. Its compressibility modifies the hydroacoustic characteristics of the hydraulic system and makes the high load instability disappear. After the start-up, the loading and the stop of the unit, the air volume has been expelled and therefore the instability reappears. Hence, when the main inlet valve of unit 2 is re-opened, it does not allow to suppress the high load instability anymore since the air volume disappeared.

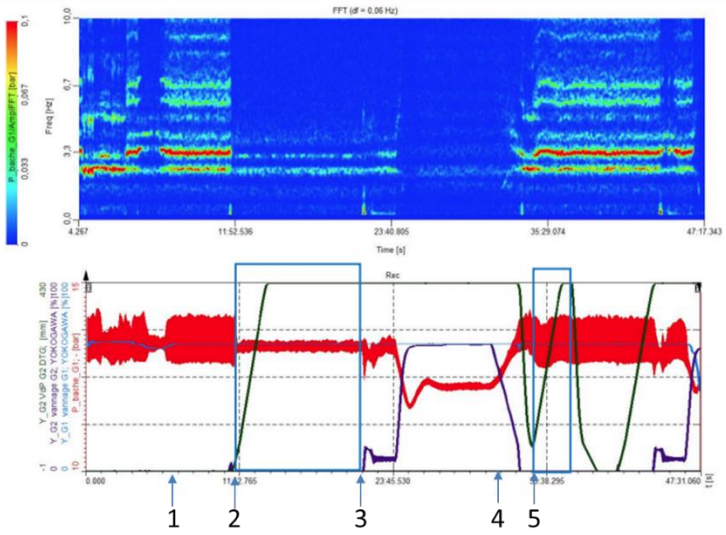

Figure 12 Time-frequency diagram (Top) and corresponding time evolution (Bottom) of spiral case pressure fluctuations (red), main inlet valve opening (green) and guide vane opening (purple).

To confirm this explanation, an air volume has been implemented in the SIMSEN numerical model of the power plant downstream to the main inlet valve. An air volume of 0.5 m3 is considered and the resulting 3DT eigenmode with air volume is represented in Figure 13 and compared to the case without air volume. It can be observed that pressure fluctuations amplitudes in the penstock are strongly reduced whereas amplitudes in the draft tube are remaining. However, the damping is still predicted as positive.

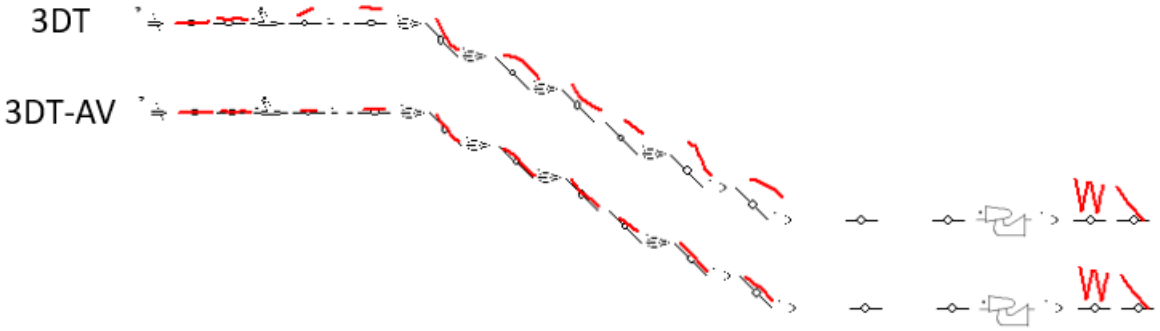

Figure 13 Shapes of draft tube pressure fluctuations amplitudes of the 3DT unstable eigenmode with air volume (3DT-AV) compared to the case without air volume (3DT).

7. Conclusion

The 15 MW power plant of Monceaux-la-Virole in France, composed of two units fed by a single penstock, experiences full-load surge. A 1D SIMSEN model of the power plant has been implemented including an advanced draft tube modelling taking into account distributed wave speed, convective terms and divergent geometry. Based on this 1D model, stability analysis by computing eigenmodes of the powerplant has been carried out and the existence of draft tube and penstock eigenmodes has been highlighted. Penstock eigenmodes are predicted stable and frequencies do not depend on draft tube wave speed parameter. Whereas spatial shapes and frequency of pressure fluctuations of draft tube eigenmodes vary as function of the wave speed and may become unstable when low draft tube wave speed values are experienced. Combined with the stability analysis, on-site measurements of pressure fluctuations in the penstock led to the conclusion that full load unstable phenomenon corresponds to an excitation of the penstock eigenmode by a draft tube eigenmode becoming unstable due to critical wave speed value reached. When a matching occurs between penstock eigenfrequency and unstable draft tube eigenmode frequency, high load surge phenomenon is experienced in the whole hydraulic system. At Monceaux-la-Virole power plant, this interaction occurs between the third draft tube eigenmode with the fourth or the third penstock eigenmode depending on the operating point.

8. References

[1] Jacob, T., Prénat, J.E.,Vullioud, G., Lopez, B. (1992). Surging of 140 MW Francis turbines at high load, analysis and solution. Proc. 16th IAHR Symposium on Hydraulic Machinery and Cavitation: Progress in Technology, Sao Paulo, Brazil.

[2] Koutnik, J., Nicolet, C., Schohl, G.A., Avellan, F. (2006). Overload surge event in a pumped storage power plant. Proc. 23rd IAHR Symposium on Hydraulic Machinery and Systems, Yokohama, Japan. Paper N◦ 135.

[3] Doerfler, P.K. (1985). Francis turbine surge prediction and prevention. Proc. Waterpower 85, 952–961, ASCE.

[4] Prénat, J.-E., Jacob, T. (1986). High load behavior of a Francis turbine model and scale effects. Proc. 13th IAHR Symposium on Hydraulic Machinery and Cavitation: Progress in Technology, Montréal, Canada.

[5] J. Héraud, B.Lecomte; M. Comelli; PY Lowys, G. Pavic, Empirical findings on the transmission of draft tube instabilities along the penstocks of hydraulic plants, in: Proc. of the 28th IAHR Symposium on Hydraulic Machinery and Systems, Kyoto, 2018

[6] A. Müller, Physical Mechanisms Governing Self-Excited Pressure Oscillations in Francis Turbines (Ph.D. thesis), EPFL, IGM, Lausanne, 2014

[7] Brennen, C., Acosta, A. (1976). The dynamic transfer function for a cavitating inducer. *J. Fluids Eng.* 98, 182–191.

[8] Duttweiler, M.E., Brennen, C. (2002). Surge instability on a cavitating propeller. *J. Fluid Mech.* 458, 133–152.

[9] Chen, C., Nicolet, C., Yonezawa, K., Farhat, M., Avellan, F., Tsujimoto, Y. (2008). One dimensional analysis of full load draft tube surge. *J. Fluids Eng.* 130, 041106-1–6.

[10] S. Alligne, C. Nicolet, Y. Tsujimoto, F. Avellan, Cavitation surge modelling in Francis turbine draft tube, J. Hydraul. Res. 52 (3) (2014) 399–411

[11] J.G. Pereira, E. Vagnoni , A. Favrel, C. Landry S. Alligné , C. Nicolet, F. Avellan, Prediction of unstable full load conditions in a Francis turbine prototype, *J. Mechanical Systems and Signal Processing. 169 (2014) 108666*

[12] A. Favrel, J. Gomes Pereira Jr., C. Landry, S. Alligné, L. Andolfatto, C. Nicolet, A. Avellan, Prediction of hydro-acoustic resonances in hydropower plants by a new approach based on the concept of swirl number, *J. Hydraul. Res.* (2019) 1–18,

[13] D. Chirkov, S. Cherny, P. Scherbakov, A. Zakharov, Evaluation of range of stable operation of hydraulic turbine based on 1D-3D model of full load pulsations, in: Proc. of the 6th IAHR Int. Meeting of the Workgroup on Cavitation and Dynamic Problems in Hydraulic Machinery and Systems, 2015.

[14] P. Dörfler, M. Keller, O. Braun, Francis full-load surge mechanism identified by unsteady 2-phase CFD, in: IOP Conference Series: Earth and Environmental Science, Vol. 12, IOP Publishing, 2010, 012026.

[15] J. Wack, S. Riedelbauch, Two-phase simulations of the full load surge in Francis turbines, in: IOP Conference Series: Earth and Environmental Science, Vol. 49, IOP Publishing, 2016, 092004.

[16] J. Decaix, A. Müller, A. Favrel, F. Avellan, C. Münch, URANS models for the simulation of full load pressure surge in Francis turbines validated by particle image velocimetry, J. Fluids Eng. 139 (12) (2017) 121103.

[17] Nicolet, C. (2007). Hydroacoustic modeling and numerical simulation of unsteady operation of hydroelectric systems. *PhD Thesis N◦ 3751*. EPFL, Lausanne, Switzerland.

[18] P.K. Dörfler, Pressure wave propagation and damping in a long penstock, in: 4th International Meeting on Cavitation and Dynamic Problems in Hydraulic and Systems, Serbia, 2011.